

Decentralized Deep Learning with Arbitrary Communication Compression

Anastasia Koloskova*
EPFL

Tao Lin*
EPFL

Sebastian U. Stich
EPFL

Martin Jaggi
EPFL

{anastasia.koloskova, tao.lin, sebastian.stich, martin.jaggi}@epfl.ch

Abstract

Decentralized training of deep learning models is a key element for enabling data privacy and on-device learning over networks, as well as for efficient scaling to large compute clusters. As current approaches suffer from limited bandwidth of the network, we propose the use of communication compression in the decentralized training context. We show that CHOCO-SGD—recently introduced and analyzed for strongly-convex objectives only—converges under arbitrary high compression ratio on general *non-convex* functions at the rate $\mathcal{O}(1/\sqrt{nT})$ where T denotes the number of iterations and n the number of workers. The algorithm achieves linear speedup in the number of workers and supports higher compression than previous state-of-the-art methods. We demonstrate the practical performance of the algorithm in two key scenarios: the training of deep learning models (i) over distributed user devices, connected by a social network and (ii) in a datacenter (outperforming all-reduce time-wise).

1 Introduction

Distributed machine learning—i.e. the training of machine learning models using distributed optimization algorithms—has enabled many recent successful applications in research and industry. Existing methods are typically based on data-parallel stochastic gradient descent (SGD), and exchange model weights or gradients over a communication network during training. Such methods offer two of the key success factors: 1) *computational scalability* by leveraging the simultaneous computational power of many devices, and 2) *data-locality*, the ability to perform joint training while keeping each part of the training data local to each participating device.

A main down-side of existing methods is their reliance on communication schemes which are centralized, and thus often lack robustness, privacy and communication efficiency. Specifically, such schemes either impose congestion on the central coordinator or parameter server (n -to-1 communication) or take significant time ($\mathcal{O}(\log n)$ for all-reduce operations).

In contrast, decentralized training algorithms such as e.g. (Lian et al., 2017; Assran et al., 2019) are free of any central coordinator, and alleviate some of these main concerns. More specifically, in the decentralized setting, all devices only perform local communication with their neighboring nodes in the given network topology, which makes such schemes much more communication efficient, as the degrees of the nodes are often just small constants (e.g. on a ring or torus), independent of the number of devices n . Additionally, recent theoretical results indicate that decentralized schemes can be as efficient as the centralized approaches, at least when considering convergence of training loss vs. iterations (Scaman et al., 2017, 2018; Koloskova et al., 2019; Tang et al., 2018; Lian et al., 2017).

To reduce the amount of data that has to be sent over each communication link, gradient compression techniques have been proposed for the standard distributed training case (Alistarh et al., 2017; Wen et al., 2017; Lin et al., 2018b; Wangni et al., 2018; Stich et al., 2018). For decentralized training of deep neural networks the pioneering work (Tang et al., 2018) introduced two algorithms (DCD, ECD) which allow communication compression. However, both these algorithms are restrictive with respect to the used compression operators, only allowing for unbiased compressors and—more significantly—so far not supporting arbitrarily high compression ratios.

*Equal contribution.

As remedy, we translate the recently proposed CHOCO-SGD (Koloskova et al., 2019) algorithm to the non-convex setting and provide a concise convergence analysis. The method allows the use of a much richer class of compression operators (such as arbitrary low quantization, sparsification, etc.), but has only been analyzed in the strongly-convex setting so far.

Contributions. Our contributions can be summarized as:

- We show that CHOCO-SGD converges at rate $\mathcal{O}(1/\sqrt{nT} + n/(\rho^4\delta^2T))$ on non-convex smooth functions, where n denotes the number of nodes, T the number of iterations, ρ the spectral gap of the mixing matrix and δ the compression ratio. The main term, $\mathcal{O}(1/\sqrt{nT})$, matches with the centralized baselines with exact communication and shows a linear speedup in the number of workers n . Both ρ and δ only affect the asymptotically smaller second term. CHOCO-SGD is the first decentralized algorithm that converges for arbitrary high compression (i.e. arbitrary small $\delta > 0$) and achieves linear speedup.
- On the practical side, we demonstrate the strong performance of the algorithm in two relevant scenarios, firstly for *on-device training* over a realistic distributed social network, where lowering the bandwidth requirements of joint training is especially impactful, and secondly for *computational scalability* of training deep learning models in a datacenter setting for resource efficiency and time-to-accuracy.
- We are able to incorporate momentum into the decentralized algorithm, and analyze its practical performance. As generalization error is of utmost importance in deep learning applications, we demonstrate training as well as test error for our methods in comparison to centralized baselines.

2 Related Work

Algorithms based on stochastic gradient descent (SGD) (Robbins and Monro, 1951; Bottou, 2010) and its mini-batch variant (Dekel et al., 2012) are most prominently used for the training of deep learning models (Goyal et al., 2017). For the training in communication restricted settings a variety of modifications have been proposed. For instance, decentralized schemes (Lian et al., 2017), gradient compression (Alistarh et al., 2017; Wen et al., 2017; Lin et al., 2018b), asynchronous methods (Recht et al., 2011; Assran et al., 2019) or performing multiple local SGD steps before averaging (Zhang et al., 2016; McMahan et al., 2017; Lin et al., 2018a). The latter two approaches are complementary to the techniques considered in this paper, which advocates for combining the first two, i.e. decentralized SGD schemes with gradient compression.

Decentralized SGD. Various schemes for decentralized optimization have been developed in the control and optimization literature. For a comprehensive overview we refer to e.g. (Nedić et al., 2018; Koloskova et al., 2019) and the references therein. We here in particular focus on approaches based on gossip averaging (Kempe et al., 2003; Xiao and Boyd, 2004; Boyd et al., 2006) whose convergence rate typically depends on the spectral gap $\rho \geq 0$ of the mixing matrix (Xiao and Boyd, 2004). Lian et al. (2017) combine SGD with gossip averaging and show convergence at the rate $\mathcal{O}(1/\sqrt{nT} + n/(\rho^2T))$. The leading term in the rate, $\mathcal{O}(1/\sqrt{nT})$, is consistent with the convergence of the centralized mini-batch SGD (Dekel et al., 2012) and the spectral gap only affects the asymptotically smaller terms. Similar results have been observed very recently for schemes with momentum (Yu et al., 2019) and previously also for decentralized optimization in the convex setting (Scaman et al., 2017, 2018; Koloskova et al., 2019).

Quantization. Communication compression with quantization has been popularized in the deep learning community by the reported successes in (Seide et al., 2014; Strom, 2015). Theoretical guarantees were first established for schemes with unbiased compression (Alistarh et al., 2017; Wen et al., 2017; Wangni et al., 2018) but soon extended to biased compression (Bernstein et al., 2018) as well. Schemes with error correction work often best in practice and give the best theoretical guarantees (Lin et al., 2018b; Alistarh et al., 2018; Stich et al., 2018; Karimireddy et al., 2019). Recently, also proximal updates and variance reduction have been studied in combination with quantized updates (Mishchenko et al., 2019; Horváth et al., 2019). We here measure the compression quality of the schemes by a parameter $\delta \in [0, 1]$, $\delta = 1$ meaning no compression, adapting the notation from e.g. (Tang et al., 2018; Stich et al., 2018).

Decentralized Optimization with Quantization. It has been observed that gossip averaging can diverge (or not converge to the correct solution) in the presence of quantization noise (Xiao et al., 2005; Carli et al., 2007; Nedić et al., 2008; Dimakis et al., 2010; Carli et al., 2010b; Yuan et al., 2012). Reisizadeh et al. (2018a) propose an algorithm that can still converge, though at a slower rate than the exact scheme. Another line of work proposed adaptive schemes (with increasing compression accuracy) that converge at the expense of higher communication cost (Carli et al., 2010a; Doan et al., 2018; Berahas et al., 2019). For deep learning applications, Tang et al. (2018) proposed the DCD algorithm that converges at the same rate than the centralized baseline, $\mathcal{O}(1/\sqrt{nT} + n/(\rho^2 T))$, though only for quantization with quality $\delta = \max\{1 - \Theta(\rho^2), 1/4\}$, which may be limiting (not allowing the for the desired compression ratio) on many network topologies (e.g. $\rho = \Theta(1/n^2)$ for a ring topology, or $\rho = \Theta(1/n)$ for a torus (Aldous and Fill, 2002, p. 169)). To address this issue, Tang et al. (2018) further propose ECD which is analyzed for a different class of compression operators (absolute measure of the quantization error) and appears less stable in experiments.¹ The CHOCO-SGD algorithm that we consider in this work has been introduced in (Koloskova et al., 2019) and analyzed for strongly convex functions with no restrictions on δ . For non-convex functions we show a rate of $\mathcal{O}(1/\sqrt{nT} + n/(\rho^4 \delta^2 T))$. The dependence of the rate on ρ is worse than for the baselines, but the algorithm converges under arbitrary bandwidth constraints $\delta > 0$.

3 CHOCO-SGD

In this section we formally introduce the decentralized optimization problem, compression operators, and the gossip-based stochastic optimization algorithm CHOCO-SGD from (Koloskova et al., 2019).

Distributed Setup. We consider optimization problems distributed across n nodes of the form

$$f^* := \min_{\mathbf{x} \in \mathbb{R}^d} \left[f(\mathbf{x}) := \frac{1}{n} \sum_{i=1}^n f_i(\mathbf{x}) \right], \quad f_i := \mathbb{E}_{\xi_i \sim D_i} F_i(\mathbf{x}, \xi_i), \quad \forall i \in [n], \quad (1)$$

where D_1, \dots, D_n are local data distributions which can be different on every node, $F_i: \mathbb{R}^d \times \Omega \rightarrow \mathbb{R}$ are possibly non-convex loss functions. This setting covers the important case of empirical risk minimization in distributed machine learning and deep learning applications.

Communication. Every device is only allowed to communicate with its local neighbours defined by the network *topology*. Formally, we define communication graph $G = ([n], E)$, with edges E representing the communication links along which messages (e.g. model updates) can be exchanged. We assign a positive weight w_{ij} to every edge ($w_{ij} = 0$ for disconnected nodes $\{i, j\} \notin E$) and impose the following (standard) assumptions on the mixing weights:

Assumption 1 (Mixing matrix). *We assume that $W \in [0, 1]^{n \times n}$, $(W)_{ij} = w_{ij}$ is a symmetric ($W = W^\top$) doubly stochastic ($W\mathbf{1} = \mathbf{1}, \mathbf{1}^\top W = \mathbf{1}^\top$) matrix with eigenvalues $1 = |\lambda_1(W)| > |\lambda_2(W)| \geq \dots \geq |\lambda_n(W)|$ and spectral gap $\rho := 1 - |\lambda_2(W)| \in (0, 1]$.*

For any connected network topology there are infinitely many weights that satisfy Assumption 1. However, to achieve fastest mixing, the spectral gap ρ should be as large as possible. This design problem can be cast as a semidefinite optimization problem (Xiao and Boyd, 2004) but a common heuristic is to set the weights based on the local node degrees: $w_{ij} = \max\{\deg(i), \deg(j)\}^{-1}$ for $\{i, j\} \in E$. This will not only guarantee $\rho > 0$ but these weights can easily be computed in a local fashion on each node (Xiao and Boyd, 2004). We adopt this choice for all our experiments.

Compression. We aim to only transmit *compressed* (e.g. quantized or sparsified) messages. We formalized this through the notion of compression operators that was e.g. also used in (Tang et al., 2018; Stich et al., 2018).

Definition 3.1 (Compression operator). *$Q: \mathbb{R}^d \rightarrow \mathbb{R}^d$ is a compression operator if it satisfies*

$$\mathbb{E}_Q \|Q(\mathbf{x}) - \mathbf{x}\|^2 \leq (1 - \delta) \|\mathbf{x}\|^2, \quad \forall \mathbf{x} \in \mathbb{R}^d, \quad (2)$$

for a parameter $\delta > 0$. Here \mathbb{E}_Q denotes the expectation over the internal randomness of operator Q .

¹ Whilst absolute bounds on the quantization error are sometimes considered in the literature (Reisizadeh et al., 2018b; Tang et al., 2018) these bounds might be restrictive (i.e. allowing only for low compression) when the input vectors are unbounded. This might be the reason for the instabilities observed in (Tang et al., 2018, Fig. 4), (Koloskova et al., 2019, Figs. 5–6).

Algorithm 1 CHOCO-SGD (Koloskova et al., 2019)

input: Initial values $\mathbf{x}_i^{(0)} \in \mathbb{R}^d$ on each node $i \in [n]$, consensus stepsize γ , SGD stepsize η , communication graph $G = ([n], E)$ and mixing matrix W , initialize $\hat{\mathbf{x}}_i^{(0)} := \mathbf{0} \forall i \in [n]$

- 1: **for** t **in** $0 \dots T-1$ **do** *{in parallel for all workers $i \in [n]$ }*
- 2: $\mathbf{x}_i^{(t)} := \mathbf{x}_i^{(t-\frac{1}{2})} + \gamma \sum_{j: \{i,j\} \in E} w_{ij} (\hat{\mathbf{x}}_j^{(t)} - \hat{\mathbf{x}}_i^{(t)})$ \triangleleft modified gossip averaging
- 3: $\mathbf{q}_i^{(t)} := Q(\mathbf{x}_i^{(t)} - \hat{\mathbf{x}}_i^{(t)})$ \triangleleft compression
- 4: **for** neighbors $j: \{i, j\} \in E$ (including $\{i\} \in E$) **do**
- 5: Send $\mathbf{q}_i^{(t)}$ and receive $\mathbf{q}_j^{(t)}$ \triangleleft communication
- 6: $\hat{\mathbf{x}}_j^{(t+1)} := \mathbf{q}_j^{(t)} + \hat{\mathbf{x}}_j^{(t)}$ \triangleleft local update
- 7: **end for**
- 8: Sample $\xi_i^{(t)}$, compute gradient $\mathbf{g}_i^{(t)} := \nabla F_i(\mathbf{x}_i^{(t)}, \xi_i^{(t)})$
- 9: $\mathbf{x}_i^{(t+\frac{1}{2})} := \mathbf{x}_i^{(t)} - \eta \mathbf{g}_i^{(t)}$ \triangleleft stochastic gradient update
- 10: **end for**

In contrast to the quantization operators used in e.g. (Alistarh et al., 2017; Horváth et al., 2019), compression operators defined as in (2) are not required to be unbiased and therefore supports a larger class of compression operators. Some examples can be found in (Koloskova et al., 2019) and we further discuss specific compression schemes in Section 5.

Algorithm. CHOCO-SGD is summarized in Algorithm 1. Every worker i stores its own private variable $\mathbf{x}_i \in \mathbb{R}^d$ that is updated by a stochastic gradient step in part ② and a modified gossip averaging step on line 2. This step is a key element of the algorithm as it preserves the averages of the iterates even in presence of quantization noise (the compression errors are not discarded, but aggregated in the local variables \mathbf{x}_i , see also (Koloskova et al., 2019)). The nodes communicate with their neighbors in part ① and update the variables $\hat{\mathbf{x}}_j \in \mathbb{R}^d$ for all their neighbors $\{i, j\} \in E$ only using compressed updates. The ‘publicly available’ copies $\hat{\mathbf{x}}_i$ are identical on all nodes, but in general $\mathbf{x}_i \neq \hat{\mathbf{x}}_i$, due to the communication restrictions.

From an implementation aspect, it is worth highlighting that the communication part ① and the gradient computation part ② can both be executed in parallel because they are independent.

4 Convergence of CHOCO-SGD on Smooth Non-Convex Problems

As the first main contribution, we here extend the analysis of CHOCO-SGD to non-convex problems. For this we make the following technical assumptions:

Assumption 2. Each function $f_i: \mathbb{R}^d \rightarrow \mathbb{R}$ for $i \in [n]$ is L -smooth, that is

$$\|\nabla f_i(\mathbf{y}) - \nabla f_i(\mathbf{x})\| \leq L \|\mathbf{y} - \mathbf{x}\|, \quad \forall \mathbf{x}, \mathbf{y} \in \mathbb{R}^d, i \in [n],$$

and the variance of the stochastic gradients is bounded on each worker:

$$\mathbb{E}_{\xi_i} \|\nabla F_i(\mathbf{x}, \xi_i) - \nabla f_i(\mathbf{x})\|^2 \leq \sigma_i^2, \quad \mathbb{E}_{\xi_i} \|\nabla F_i(\mathbf{x}, \xi_i)\|^2 \leq G^2, \quad \forall \mathbf{x} \in \mathbb{R}^d, i \in [n], \quad (3)$$

where $\mathbb{E}_{\xi_i}[\cdot]$ denotes the expectation over $\xi_i \sim \mathcal{D}_i$. We also denote $\bar{\sigma}^2 := \frac{1}{n} \sum_{i=1}^n \sigma_i^2$ for convenience.

The smoothness assumption is crucial for the analysis as it controls how fast the function values can change locally. The bounded variance assumption is standard in the stochastic optimization literature. We now state the main result of this section:

Theorem 4.1. Under Assumptions 1–2, with constant stepsize $\eta = \sqrt{n}/\sqrt{T+1}$ and the consensus stepsize from (Koloskova et al., 2019), $\gamma := \frac{\rho^2 \delta}{16\rho + \rho^2 + 4\beta^2 + 2\rho\beta^2 - 8\rho\delta}$ with $\beta = \|I - W\|_2 \in [0, 2]$, and $T \geq 64nL^2$, the averaged iterates $\bar{\mathbf{x}}^{(t)} := \frac{1}{n} \sum_{i=1}^n \mathbf{x}_i^{(t)}$ of Algorithm 2 satisfy:

$$\frac{1}{T+1} \sum_{t=0}^T \left\| \nabla f(\bar{\mathbf{x}}^{(t)}) \right\|_2^2 \leq \frac{4(f(\bar{\mathbf{x}}^{(0)}) - f^*) + 4\bar{\sigma}^2 L}{\sqrt{n(T+1)}} + \frac{24G^2 nL}{c^2(T+1)},$$

where $c := \frac{\rho^2 \delta}{82}$ denotes the convergence rate of the underlying consensus averaging scheme of (Koloskova et al., 2019).

This result shows that CHOCO-SGD converges asymptotically as $\mathcal{O}(1/\sqrt{nT} + n/(\rho^4 \delta^2 T))$. The first term shows a linear speed-up compared to SGD on a single node, while compression and graph topology affect only the higher order second term. However, comparing the second term with the corresponding term in the convergence rate of the centralized baseline with exact communication we see that they differ by a factor of $(\rho\delta)^2$. The dependence on δ is a consequence of supporting arbitrary high compression, but the superfluous ρ^2 term seems to be a consequence of the analysis (only for the special case of $\delta = 1$ we recover $\mathcal{O}(n/(\rho^2 T))$ as the second term. This is shown in the appendix.). For slightly more general statements than Theorem 4.1 (with improved constants) as well as for the proofs we refer to Appendix A.

The theorem gives guarantees for the averaged vector of parameters $\bar{\mathbf{x}}$, however in a decentralized setting it is very expensive and sometimes impossible to average all the parameters distributed across several machines, especially when the number of machines and the model size is large. We can get similar guarantees on the individual iterates \mathbf{x}_i as e.g. in (Assran et al., 2019). We summarize these briefly below.

Lemma 4.2. *Under the same setting as in Theorem 4.1, the iterates of Algorithm 1 satisfy:*

$$\frac{1}{n} \sum_{i=1}^n \left\| \bar{\mathbf{x}}^{(t)} - \mathbf{x}_i^{(t)} \right\|_2^2 \leq \frac{8nG^2}{c^2(T+1)}.$$

Corollary 4.3 (Convergence of local weights). *Under the same setting as in Theorem 4.1,*

$$\frac{1}{T+1} \sum_{t=0}^T \frac{1}{n} \sum_{i=1}^n \left\| \nabla f(\mathbf{x}_i^{(t)}) \right\|_2^2 \leq \frac{8(f(\bar{\mathbf{x}}^{(0)}) - f^*) + 8\bar{\sigma}^2 L}{\sqrt{n(T+1)}} + \frac{64G^2 nL}{c^2(T+1)}.$$

For the proofs of these statements we again refer to Appendix A. This corollary means that sequence $\mathbf{x}_i^{(t)}$ at uniformly chosen worker i in expectation converges with the same rate (up to constants) as sequence of averaged vectors $\bar{\mathbf{x}}^{(t)}$ over the workers.

5 Comparison to Baselines for Various Compression Schemes

In this section we experimentally compare CHOCO-SGD to the relevant baselines for a selection of commonly used compression operators. For the experiments we further leverage momentum in all implemented algorithms. The newly developed momentum version of CHOCO-SGD is given as Algorithm 3 in Appendix D.

Setup. In order to match the setting in (Tang et al., 2018) for our first set of experiments, we use a ring topology with $n = 8$ nodes and train the **ResNet20** architecture (He et al., 2016) on the **Cifar10** dataset (50K/10K training/test samples) (Krizhevsky, 2012). We randomly split the training data between workers and shuffle it after every epoch, following standard procedure as e.g. in (Goyal et al., 2017). We implement DCD and ECD with momentum (Tang et al., 2018), CHOCO-SGD with momentum (Algorithm 3) and standard (all-reduce) mini-batch SGD with momentum and without compression (Dekel et al., 2012). The momentum factor is set to 0.9 without dampening. For all algorithms we fine-tune the initial learning rate and gradually warm it up from a relative small value (0.1) (Goyal et al., 2017) for the first 5 epochs. The learning rate is decayed by 10 twice, at 150 and 225 epochs, and stop training at 300 epochs. For CHOCO-SGD the consensus learning rate γ is also tuned. The detailed hyper-parameter tuning procedure refers to Appendix E. Every compression scheme is applied to every layer of **ResNet20** separately. We evaluate the top-1 accuracy on every node separately over the whole dataset and report the average performance over all nodes (the same performance measure scheme is also used in the following sections).

Table 1: Top-1 test accuracy for decentralized DCD, ECD and CHOCO-SGD with different compression schemes. Reported top-1 test accuracies are averaged over three runs with fine-tuned hyper-parameters (learning rate, weight decay, consensus stepsize). The fine-tuned all-reduce baseline reaches accuracy 92.64, with 1.04 MB gradient transmission per iteration. (* indicates that 2 out of 3 runs diverged).

Algorithm	Quantization (QSGD)				Sparsification (random-%)		
	16 bits	8 bits	4 bits	2 bits	50%	10%	1%
quantization level							
transmitted data/iteration	0.52 MB	0.26 MB	0.13 MB	0.065 MB	1.04 MB	0.21 MB	0.031 MB
DCD-PSGD	92.51 \pm 0.05	92.36 \pm 0.28	23.56 \pm 2.97	diverges	92.05 \pm 0.25	diverges	diverges
ECD-PSGD	92.02 \pm 0.14	59.11 \pm 1.57	diverges	diverges	diverges	diverges	diverges
CHOCO-SGD	92.34 \pm 0.19	92.30 \pm 0.08	91.92 \pm 0.27	91.41 \pm 0.11	92.54 \pm 0.26	91.87 \pm 0.21	91.32 \pm 0.17

Algorithm	Sparsification (top-%)			Sign+Norm
	50%	10%	1%	
quantization level				-
transmitted data/iteration	1.04 MB	0.21 MB	0.031 MB	0.032 MB
DCD-PSGD	92.40 \pm 0.11	91.97 \pm 0.14	89.79 \pm 0.40	92.40 \pm 0.14
ECD-PSGD	17.03 *	16.78 *	18.03 *	diverges
CHOCO-SGD	92.54 \pm 0.26	92.29 \pm 0.05	91.73 \pm 0.11	92.46 \pm 0.10

Compression Schemes. We implement two *unbiased* compression schemes:

- gsgd_b quantization that randomly rounds the weights to b -bit representations (Alistarh et al., 2017), and
- random_a sparsification, which preserves a randomly chosen a fraction of the weights and sets the other ones to zero (Wangni et al., 2018).

Further two *biased* compression schemes:

- top_a , which selects the a fraction of weights with the largest magnitude and sets the other ones to zero (Alistarh et al., 2018; Stich et al., 2018), and
- sign compression, which compresses each weight to its sign scaled by the norm of the full vector (Bernstein et al., 2018; Karimireddy et al., 2019).

We refer to Appendix C for exact definitions of the schemes.

DCD and ECD have been analyzed only for unbiased quantization schemes, thus the combination with the two biased schemes is not supported by theory. In converse, CHOCO-SGD has been studied only for biased schemes according to Definition 2. However, both unbiased compression schemes can be scaled down in order to meet the specification (cf. discussions in (Stich et al., 2018; Koloskova et al., 2019)) and we adopt this for the experiments.

Results. The results are summarized in Table 1. For unbiased compression schemes, ECD and DCD only achieve good performance when the compression ratio is small, and sometimes even diverge when the compression ratio is high. This is consistent with the theoretical and experimental results in (Tang et al., 2018). We further observe that the performance of DCD with the biased top_a sparsification is much better than with the unbiased random_a counterpart, though this operator is not yet supported by theory.

CHOCO-SGD can generalize reasonably well in all scenarios (at most 1.65% accuracy drop) for fixed training budget. The sign compression achieves state-of-the-art accuracy and requires approximately $32\times$ less bits per weight than the full precision baseline.

6 Use case I: On-device Learning over a Social Network Graph

Whilst in the previous section we focused on an artificial scenario, we now shift our focus to applications that are intrinsically decentralized, and where centralized methods either fail or are inefficient to implement. Typical scenarios comprise e.g. sensor networks, or mobile devices that jointly train a machine learning model, based on use feedback each device. These devices could either be linked in a cellphone network topology, over the internet, or in a social network graph. Common to these applications is that i) the network topology is fixed and the global topology is typically unknown to a single device, ii) each device has only access to locally stored or acquired data and iii) the bandwidth is limited (either physically, or artificially for e.g. metered connections). Additionally, this fully decentralized setting is also strongly motivated by privacy aspects, benefitting from keeping private training data on-device at all times.

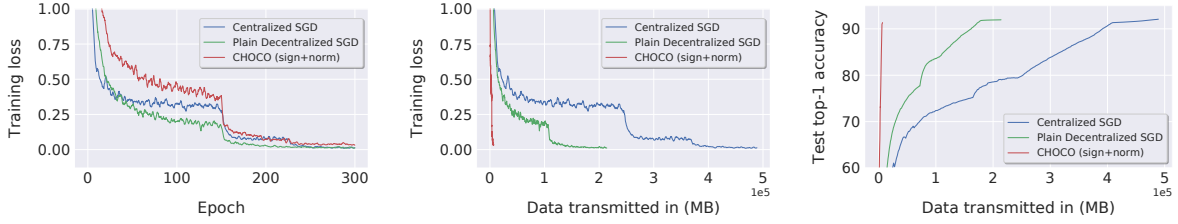


Figure 1: Image classification: ResNet-20 on CIFAR-10 on social network topology.

Modeling. To simulate this scenario, we evaluate the algorithms on a real social network topology, we chose the “Davis Southern women social network” (Davis et al., 1941) with 89 edges between $n = 32$ nodes (max degree 14, $\rho = 0.068$). We randomly split the training data between the nodes and keep this partition fixed during the entire training (no shuffling). As mixing weights in decentralized setting we resort to the locally computable weights that were introduced in Section 3. As gathering methods such as all-reduce are not efficiently implementable in this scenario, we compare to the centralized baseline where all nodes route their updates to a central coordinator for aggregation.

Setup. For the comparison we consider CHOCO-SGD with sign compression (this combination achieved the compromise between accuracy and compression level in Table 1), decentralized SGD without compression, and centralized SGD without compression. We train two models, firstly **ResNet20** (He et al., 2016) (0.27 million parameters) for image classification on the **Cifar10** dataset (50K/10K training/test samples) (Krizhevsky, 2012) and secondly, a three-layer **LSTM** architecture (Hochreiter and Schmidhuber, 1997) (28.95 million parameters) for a language modeling task on WikiText-2 (600 training and 60 validation articles with a total of 2’088’628 and 217’646 tokens respectively) (Merity et al., 2016). For the language modeling task, we borrowed and adapted the general experimental setup of (Merity et al., 2017), where we use a three-layer LSTM with hidden dimension of size 650. The loss is averaged over all examples and timesteps. The BPTT length is set to 30. We fine-tune the value of gradient clipping (0.4), and the dropout (0.4) is only applied on the output of LSTM.

We train both of **ResNet20** and **LSTM** for 300 epochs, unless mentioned specifically. The per node mini-batch size is 32 for both datasets. The learning rate of CHOCO-SGD follows a linear scaling rule, which is proportional to the node degree. We fine-tune the base learning rate (before the linear scaling) and gradually warm it up (from 0.1) for the first 5 training epochs. The scaled learning rate will be decayed by the factor of 10 at the phase when the training algorithm has accessed 50% and 75% of the total training epochs. The momentum (with factor 0.9) is only applied on the **ResNet20** training.

Results. The results are summarized in Figures 1–2 and in Table 2. For the image classification task, when comparing the training accuracy reached after the same number of epochs, we observe that the decentralized algorithm performs best, follows by the centralized and lastly the quantized decentralized. However, the test accuracy is highest for the centralized scheme. When comparing the test accuracy reached for the same transmitted data², CHOCO-SGD significantly outperforms the exact decentralized scheme, with the centralized performing worst. We note a slight accuracy drop, i.e. after the same number of epochs (but much less transmitted data), CHOCO-SGD does not reach the same level of test accuracy than the baselines.

For the language modeling task, both decentralized schemes suffer a drop in the training loss when the evaluation reaching the epoch budget; while our CHOCO-SGD outperforms the centralized SGD in test perplexity. When considering perplexity for a fixed data volume (middle and right subfigure of Figure 2), CHOCO-SGD performs best, followed by the exact decentralized and centralized algorithms.

7 Use case II: Efficient Large-Scale Training in a Datacenter Setting

Decentralized optimization methods offer a way to address scaling issues even for well connected devices, such as e.g. in datacenter with fast InfiniBand (100Gbps) or Ethernet (10Gbps) connections. Lian et al. (Lian et al., 2017) describe scenarios when decentralized schemes can outperform centralized ones, and

² The figure reports the transmitted data on the busiest node, i.e. on the max-degree node (degree 14) node for decentralized schemes, and degree 32 for the centralized one.

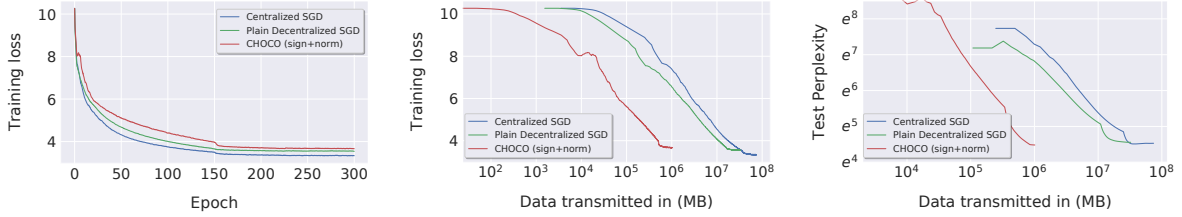


Figure 2: Language modeling: LSTM on WikiText-2 on social network topology.

Table 2: Summary of performance when training with the same epoch budget (as centralized SGD).

Algorithm	max. connections/node	ResNet-20 (Figure. 1)		LSTM (Figure. 2)	
		data/gradient	top-1 test acc.	data/gradient	test perplexity
Centralized SGD	32	1.04 MB	93.00	110.43 MB	89.39
Exact Decentralized SGD	14	1.04 MB	92.29	110.43 MB	96.33
sign-CHOCO-SGD	14	0.032 MB	91.90	3.45 MB	89.09

recently, Assran et al. (Assran et al., 2019) presented impressive speedups for training on 256 GPUs. The main differences of their algorithm to CHOCO-SGD are the asynchronous gossip updates, time-varying communication topology and most importantly exact communication, making their setup not directly comparable to ours. We note that these properties of asynchronous communication and changing topology for faster mixing are orthogonal to our contribution, and offer promise to be combined.

Setup. We train **ImageNet-1k** (1.28M/50K training/validation) (Deng et al., 2009) with **Resnet-50** (He et al., 2016). We perform our experiments on 8 machines (n1-standard-32 from Google Cloud), where each of machines has 4 Tesla P100 GPUs. Within one machine communication is fast and we perform all-reduce with the full model. Between different machines we use decentralized communication with compressed communication (sign-CHOCO-SGD) in a ring topology. The mini-batch size on each GPU is 128, and we follow the general SGD training scheme in (Goyal et al., 2017) and directly use all their hyper parameters for CHOCO-SGD. Due to the limitation of the computational resource, we did not heavily tune the consensus stepsize for CHOCO-SGD³.

Results. We depict the training loss and top-1 test accuracy in terms of epochs and time in Figure 3. CHOCO-SGD benefits from its decentralized and parallel structure and takes less time than all-reduce to perform the same number of epochs, while having only a slight 1.5% accuracy loss. (All-reduce with full precision gradients achieved test accuracy of 76.37%, vs. 75.15% for CHOCO-SGD). In terms of time per epoch, our speedup does not match that of (Assran et al., 2019), as the used hardware is very different. Their scheme is orthogonal to our approach and could be integrated for better training efficiency. Nevertheless, we still demonstrate a time-wise 20% gain over the all-reduce baseline, on our used commodity hardware cluster.

8 Discussion

We demonstrate that CHOCO-SGD can reach good accuracy in all scenarios and can provide significant savings in terms of bandwidth. However, on all tasks the final accuracy did not precisely match the respective state-of-the-art performance for well-tuned mini-batch baselines⁴. Besides suboptimal parameter choices, this is also explained by the fact that we only allocated a fixed budget in terms of epochs (total gradient computations), irrespective of graph topology and compression. If we would compare accuracy for e.g. a fixed volume of transmitted data, the picture drastically changes. We argue that this accuracy drop might still be in the tolerance for many distributed on-device applications, however not for the

³ We estimate the consensus stepsize by running CHOCO-SGD with different values for the first 3 epochs.

⁴ Note that while all compression schemes as in Section 5 are suitable for CHOCO-SGD, most cannot be implemented using all-reduce (as sign-compression needs aggregation of the norm for scaling, and sparse compression can not support incremental additive aggregation).

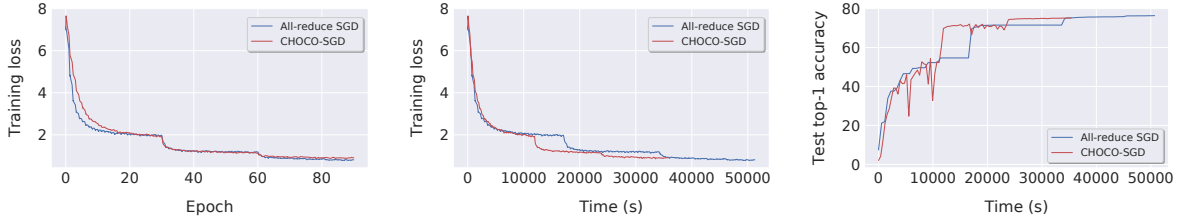


Figure 3: Large-scale training: Resnet-50 on ImageNet-1k in the datacenter setting.

datacenter scenario. There it might be possible to close the generalization gap by allowing longer training (i.e. more epochs).

Recent work reported time-wise speedups up to a factor of 3 for a decentralized method even without quantization (Assran et al., 2019). We could not obtain the same speedups with our implementation. Reasons for this are that their algorithm uses asynchronous communication and time-varying random communication graphs. In contrast, we analyzed and implemented CHOCO-SGD only for a fixed network topology, and did not leverage the internal parallelism (communication and gradient computation can be parallelized, see Section 3) in our implementation. These three modifications seem promising directions that could provide further speedups desired for industry applications. A further desirable extension of the scheme would be to allow for adaptive (or automatically tuned) consensus stepsize that could further ease the adaptation of the scheme in real applications.

9 Conclusion

We propose to use CHOCO-SGD (and its momentum version) for accelerating distributed training in bandwidth constrained environments. We provide theoretical convergence guarantees for the non-convex setting and show that the algorithm enjoys the same linear speedup as the centralized communication baseline when increasing the number of nodes. We empirically study the performance of the algorithm in a variety of settings on image classification (ImageNet-1k, Cifar20) and on a language modeling task (WikiText-2). Whilst previous work successfully demonstrated that decentralized methods are a competitive alternative to centralized training schemes for deep learning (Lian et al., 2017; Assran et al., 2019) we here significantly expand the possible applications by enabling training in strongly communication-restricted environments. We demonstrate that decentralized schemes can converge for arbitrary high communication compression and thus quantization is a meaningful way to accelerate decentralized training of deep learning models.

Acknowledgments

We acknowledge funding from SNSF grant 200021_175796, as well as a Google Focused Research Award.

References

- David Aldous and James Allen Fill. Reversible markov chains and random walks on graphs, 2002. Unfinished monograph, recompiled 2014, available at [http://www.stat.berkeley.edu/~sim\\$aldous/RWG/book.html](http://www.stat.berkeley.edu/~sim$aldous/RWG/book.html).
- Dan Alistarh, Demjan Grubic, Jerry Li, Ryota Tomioka, and Milan Vojnovic. QSGD: Communication-efficient SGD via gradient quantization and encoding. In I. Guyon, U. V. Luxburg, S. Bengio, H. Wallach, R. Fergus, S. Vishwanathan, and R. Garnett, editors, *NIPS - Advances in Neural Information Processing Systems 30*, pages 1709–1720. Curran Associates, Inc., 2017.
- Dan Alistarh, Torsten Hoefler, Mikael Johansson, Nikola Konstantinov, Sarit Khirirat, and Cedric Renggli. The convergence of sparsified gradient methods. In S. Bengio, H. Wallach, H. Larochelle, K. Grauman, N. Cesa-Bianchi, and R. Garnett, editors, *NeurIPS - Advances in Neural Information Processing Systems 31*, pages 5977–5987. Curran Associates, Inc., 2018.
- Mahmoud Assran, Nicolas Loizou, Nicolas Ballas, and Michael Rabbat. Stochastic Gradient Push for Distributed Deep Learning. *ICML 2019*, 2019.

- Albert S. Berahas, Charikleia Iakovidou, and Ermin Wei. Nested distributed gradient methods with adaptive quantized communication. *arXiv e-prints*, page arXiv:1903.08149, 2019.
- Jeremy Bernstein, Yu-Xiang Wang, Kamyar Azizzadenesheli, and Animashree Anandkumar. signSGD: Compressed optimisation for non-convex problems. In Jennifer Dy and Andreas Krause, editors, *Proceedings of the 35th International Conference on Machine Learning*, volume 80 of *Proceedings of Machine Learning Research*, pages 560–569, Stockholmssäsan, Stockholm Sweden, 10–15 Jul 2018. PMLR.
- Léon Bottou. Large-scale machine learning with stochastic gradient descent. In Yves Lechevallier and Gilbert Saporta, editors, *Proceedings of COMPSTAT’2010*, pages 177–186, Heidelberg, 2010. Physica-Verlag HD. ISBN 978-3-7908-2604-3.
- Stephen Boyd, Arpita Ghosh, Balaji Prabhakar, and Devavrat Shah. Randomized gossip algorithms. *IEEE/ACM Trans. Netw.*, 14(SI):2508–2530, June 2006. ISSN 1063-6692. doi: 10.1109/TIT.2006.874516.
- R. Carli, F. Fagnani, P. Frasca, T. Taylor, and S. Zampieri. Average consensus on networks with transmission noise or quantization. In *2007 European Control Conference (ECC)*, pages 1852–1857, July 2007. doi: 10.23919/ECC.2007.7068829.
- R. Carli, F. Bullo, and S. Zampieri. Quantized average consensus via dynamic coding/decoding schemes. *International Journal of Robust and Nonlinear Control*, 20:156–175, 2010a. ISSN 1049-8923.
- R. Carli, P. Frasca, F. Fagnani, and S. Zampieri. Gossip consensus algorithms via quantized communication. *Automatica*, 46:70–80, 2010b. ISSN 0005-1098.
- A. Davis, B. B. Gardner, and M. R. Gardner. Deep South. *University of Chicago Press, Chicago, IL.*, May 1941.
- Ofar Dekel, Ran Gilad-Bachrach, Ohad Shamir, and Lin Xiao. Optimal distributed online prediction using mini-batches. *J. Mach. Learn. Res.*, 13(1):165–202, January 2012. ISSN 1532-4435.
- J. Deng, W. Dong, R. Socher, L.-J. Li, K. Li, and L. Fei-Fei. ImageNet: A Large-Scale Hierarchical Image Database. In *CVPR09*, 2009.
- A. G. Dimakis, S. Kar, J. M. F. Moura, M. G. Rabbat, and A. Scaglione. Gossip algorithms for distributed signal processing. *Proceedings of the IEEE*, 98(11):1847–1864, Nov 2010. ISSN 0018-9219. doi: 10.1109/JPROC.2010.2052531.
- Thinh T. Doan, Siva Theja Maguluri, and Justin Romberg. Accelerating the Convergence Rates of Distributed Subgradient Methods with Adaptive Quantization. *arXiv e-prints*, art. arXiv:1810.13245, Oct 2018.
- Priya Goyal, Piotr Dollár, Ross Girshick, Pieter Noordhuis, Lukasz Wesolowski, Aapo Kyrola, Andrew Tulloch, Yangqing Jia, and Kaiming He. Accurate, large minibatch SGD: Training ImageNet in 1 hour. *arXiv preprint arXiv:1706.02677*, 2017.
- Kaiming He, Xiangyu Zhang, Shaoqing Ren, and Jian Sun. Deep residual learning for image recognition. *2016 IEEE Conference on Computer Vision and Pattern Recognition (CVPR)*, pages 770–778, 2016.
- Sepp Hochreiter and Jürgen Schmidhuber. Long short-term memory. *Neural computation*, 9:1735–80, 12 1997. doi: 10.1162/neco.1997.9.8.1735.
- Samuel Horváth, Dmitry Kovalev, Konstantin Mishchenko, Peter Richtárik, and Sebastian Urban Stich. Stochastic distributed learning with gradient quantization and variance reduction. *Technical Report*, page arXiv:1904.05115, 2019.
- Sai Praneeth Karimireddy, Quentin Rebjock, Sebastian Urban Stich, and Martin Jaggi. Error feedback fixes SignSGD and other gradient compression schemes. *Technical Report*, page arXiv:1901.09847, 2019.
- David Kempe, Alin Dobra, and Johannes Gehrke. Gossip-based computation of aggregate information. In *Proceedings of the 44th Annual IEEE Symposium on Foundations of Computer Science, FOCS ’03*, pages 482–, Washington, DC, USA, 2003. IEEE Computer Society. ISBN 0-7695-2040-5.
- Anastasia Koloskova, Sebastian Urban Stich, and Martin Jaggi. Decentralized stochastic optimization and gossip algorithms with compressed communication. *arXiv e-prints*, art. arXiv:1902.00340, 2019.
- Alex Krizhevsky. Learning multiple layers of features from tiny images. *University of Toronto*, 05 2012.

- Xiangru Lian, Ce Zhang, Huan Zhang, Cho-Jui Hsieh, Wei Zhang, and Ji Liu. Can decentralized algorithms outperform centralized algorithms? a case study for decentralized parallel stochastic gradient descent. In I. Guyon, U. V. Luxburg, S. Bengio, H. Wallach, R. Fergus, S. Vishwanathan, and R. Garnett, editors, *NIPS - Advances in Neural Information Processing Systems 30*, pages 5330–5340. Curran Associates, Inc., 2017.
- Tao Lin, Sebastian Urban Stich, Kumar Kshitij Patel, and Martin Jaggi. Don’t use large mini-batches, use local SGD. *Technical Report*, page arXiv:1808.07217, 2018a.
- Yujun Lin, Song Han, Huizi Mao, Yu Wang, and Bill Dally. Deep gradient compression: Reducing the communication bandwidth for distributed training. In *ICLR 2018 - International Conference on Learning Representations*, 2018b.
- Brendan McMahan, Eider Moore, Daniel Ramage, Seth Hampson, and Blaise Aguera y Arcas. Communication-Efficient Learning of Deep Networks from Decentralized Data. In *AISTATS 2017 - Proceedings of the 20th International Conference on Artificial Intelligence and Statistics*, pages 1273–1282, 2017.
- Stephen Merity, Caiming Xiong, James Bradbury, and Richard Socher. Pointer sentinel mixture models. *arXiv preprint arXiv:1609.07843*, 2016.
- Stephen Merity, Nitish Shirish Keskar, and Richard Socher. Regularizing and optimizing lstm language models. *arXiv preprint*, page arXiv:1708.02182, 2017.
- Konstantin Mishchenko, Eduard Gorbunov, Martin Takáč, and Peter Richtárik. Distributed learning with compressed gradient differences. *arXiv e-prints*, page arXiv:1901.09269, 2019.
- A. Nedić, A. Olshevsky, and M. G. Rabbat. Network topology and communication-computation tradeoffs in decentralized optimization. *Proceedings of the IEEE*, 106(5):953–976, May 2018. ISSN 0018-9219. doi: 10.1109/JPROC.2018.2817461.
- Angelia Nedić, Alex Olshevsky, Asuman Ozdaglar, and John N. Tsitsiklis. Distributed subgradient methods and quantization effects. In *Proceedings of the 47th IEEE Conference on Decision and Control, CDC 2008*, pages 4177–4184, 2008. ISBN 9781424431243. doi: 10.1109/CDC.2008.4738860.
- Benjamin Recht, Christopher Re, Stephen Wright, and Feng Niu. Hogwild: A lock-free approach to parallelizing stochastic gradient descent. In J. Shawe-Taylor, R. S. Zemel, P. L. Bartlett, F. Pereira, and K. Q. Weinberger, editors, *NIPS - Advances in Neural Information Processing Systems 24*, pages 693–701. Curran Associates, Inc., 2011.
- Amirhossein Reisizadeh, Aryan Mokhtari, Hamed Hassani, and Ramtin Pedarsani. An exact quantized decentralized gradient descent algorithm. *arXiv e-prints*, page arXiv:1806.11536, 2018a.
- Amirhossein Reisizadeh, Aryan Mokhtari, S. Hamed Hassani, and Ramtin Pedarsani. Quantized decentralized consensus optimization. *CoRR*, abs/1806.11536, 2018b.
- Herbert Robbins and Sutton Monro. A Stochastic Approximation Method. *The Annals of Mathematical Statistics*, 22(3):400–407, September 1951.
- Kevin Scaman, Francis Bach, Sébastien Bubeck, Yin Tat Lee, and Laurent Massoulié. Optimal algorithms for smooth and strongly convex distributed optimization in networks. In Doina Precup and Yee Whye Teh, editors, *Proceedings of the 34th International Conference on Machine Learning*, volume 70 of *Proceedings of Machine Learning Research*, pages 3027–3036, International Convention Centre, Sydney, Australia, 06–11 Aug 2017. PMLR.
- Kevin Scaman, Francis Bach, Sebastien Bubeck, Laurent Massoulié, and Yin Tat Lee. Optimal algorithms for non-smooth distributed optimization in networks. In S. Bengio, H. Wallach, H. Larochelle, K. Grauman, N. Cesa-Bianchi, and R. Garnett, editors, *NeurIPS - Advances in Neural Information Processing Systems 31*, pages 2745–2754. Curran Associates, Inc., 2018.
- Frank Seide, Hao Fu, Jasha Droppo, Gang Li, and Dong Yu. 1-bit stochastic gradient descent and its application to data-parallel distributed training of speech DNNs. In Haizhou Li, Helen M. Meng, Bin Ma, Engsiong Chng, and Lei Xie, editors, *INTERSPEECH*, pages 1058–1062. ISCA, 2014.
- Sebastian U Stich, Jean-Baptiste Cordonnier, and Martin Jaggi. Sparsified SGD with memory. In S. Bengio, H. Wallach, H. Larochelle, K. Grauman, N. Cesa-Bianchi, and R. Garnett, editors, *NeurIPS - Advances in Neural Information Processing Systems 31*, pages 4452–4463. Curran Associates, Inc., 2018.

- Nikko Strom. Scalable distributed dnn training using commodity gpu cloud computing. In *INTERSPEECH*, pages 1488–1492. ISCA, 2015.
- Hanlin Tang, Shaoduo Gan, Ce Zhang, Tong Zhang, and Ji Liu. Communication compression for decentralized training. In S. Bengio, H. Wallach, H. Larochelle, K. Grauman, N. Cesa-Bianchi, and R. Garnett, editors, *NeurIPS - Advances in Neural Information Processing Systems 31*, pages 7663–7673. Curran Associates, Inc., 2018.
- Jianqiao Wangni, Jialei Wang, Ji Liu, and Tong Zhang. Gradient sparsification for communication-efficient distributed optimization. In S. Bengio, H. Wallach, H. Larochelle, K. Grauman, N. Cesa-Bianchi, and R. Garnett, editors, *NeurIPS - Advances in Neural Information Processing Systems 31*, pages 1306–1316. Curran Associates, Inc., 2018.
- Wei Wen, Cong Xu, Feng Yan, Chunpeng Wu, Yandan Wang, Yiran Chen, and Hai Li. Terngrad: Ternary gradients to reduce communication in distributed deep learning. In I. Guyon, U. V. Luxburg, S. Bengio, H. Wallach, R. Fergus, S. Vishwanathan, and R. Garnett, editors, *NIPS - Advances in Neural Information Processing Systems 30*, pages 1509–1519. Curran Associates, Inc., 2017.
- L. Xiao, S. Boyd, and S. Lall. A scheme for robust distributed sensor fusion based on average consensus. In *IPSN 2005. Fourth International Symposium on Information Processing in Sensor Networks, 2005.*, pages 63–70, April 2005. doi: 10.1109/IPSN.2005.1440896.
- Lin Xiao and Stephen Boyd. Fast linear iterations for distributed averaging. *Systems & Control Letters*, 53(1): 65–78, 2004. ISSN 0167-6911. doi: <https://doi.org/10.1016/j.sysconle.2004.02.022>.
- Hao Yu, Rong Jin, and Sen Yang. On the Linear Speedup Analysis of Communication Efficient Momentum SGD for Distributed Non-Convex Optimization. *ICML*, May 2019.
- Deming Yuan, Shengyuan Xu, Huanyu Zhao, and Lina Rong. Distributed dual averaging method for multi-agent optimization with quantized communication. *Systems & Control Letters*, 61(11):1053 – 1061, 2012. ISSN 0167-6911. doi: <https://doi.org/10.1016/j.sysconle.2012.06.004>.
- Jian Zhang, Christopher De Sa, Ioannis Mitliagkas, and Christopher Ré. Parallel SGD: When does averaging help? *arXiv*, 2016.

A Convergence of CHOCO-SGD

In this section we present the proof of Theorem 4.1. For this, we will first derive a slightly more general statement: in Theorem A.2 we analyze CHOCO-SGD for arbitrary stepsizes η , and then derive Theorem 4.1 as a special case.

The structure of the proof follows (Koloskova et al., 2019). That is, we first show that Algorithm 1 is a special case of a more general class of algorithms (given in Algorithm 2): Observe that Algorithm 1 consists of two main components: ② the stochastic gradient update, performed locally on each node, and ① the (quantized) averaging among the nodes. We can show convergence of all algorithms of this type—i.e. stochastic gradient updates ② followed by an arbitrary averaging step ①—as long as the averaging scheme exhibits linear convergence. For the specific averaging used in CHOCO-SGD, linear convergence has been shown in (Koloskova et al., 2019) and we will use their estimate of the convergence rate of the averaging scheme.

A.1 A General Framework for Decentralized SGD with Arbitrary Averaging

For convenience, we use the following matrix notation in this subsection.

$$X^{(t)} := [\mathbf{x}_1^{(t)}, \dots, \mathbf{x}_n^{(t)}] \in \mathbb{R}^{d \times n}, \quad \bar{X}^{(t)} := [\bar{\mathbf{x}}^{(t)}, \dots, \bar{\mathbf{x}}^{(t)}] \in \mathbb{R}^{d \times n},$$

$$\partial F(X^{(t)}, \xi^{(t)}) := [\nabla F_1(\mathbf{x}_1^{(t)}, \xi_1^{(t)}), \dots, \nabla F_n(\mathbf{x}_n^{(t)}, \xi_n^{(t)})] \in \mathbb{R}^{d \times n}.$$

Decentralized SGD with arbitrary averaging is given in Algorithm 2.

Algorithm 2 DECENTRALIZED SGD WITH ARBITRARY AVERAGING SCHEME

input: $X^{(0)}$, stepsize η , averaging function $h: \mathbb{R}^{d \times n} \times \mathbb{R}^{d \times n} \rightarrow \mathbb{R}^{d \times n} \times \mathbb{R}^{d \times n}$

```

1: for  $t$  in  $0 \dots T-1$  do {in parallel for all workers  $i \in [n]$ }
② { 2:    $X^{(t+\frac{1}{2})} = X^{(t)} - \eta \partial F_i(X^{(t)}, \xi^{(t)})$                                  $\triangleleft$  stochastic gradient updates
① { 3:    $(X^{(t+1)}, Y^{(t+1)}) = h(X^{(t+\frac{1}{2})}, Y^{(t)})$                                  $\triangleleft$  blackbox averaging/gossip
4: end for

```

Assumption 3. For an averaging scheme $h: \mathbb{R}^{d \times n} \times \mathbb{R}^{d \times n} \rightarrow \mathbb{R}^{d \times n} \times \mathbb{R}^{d \times n}$ let $(X^+, Y^+) := h(X, Y)$ for $X, Y \in \mathbb{R}^{d \times n}$. Assume that h preserves the average of iterates:

$$X^+ \frac{\mathbf{1}\mathbf{1}^\top}{n} = X \frac{\mathbf{1}\mathbf{1}^\top}{n}, \quad \forall X, Y \in \mathbb{R}^{d \times n},$$

and that it converges with linear rate for a parameter $0 < c \leq 1$

$$\mathbb{E}_h \Psi(X^+, Y^+) \leq (1 - c) \Psi(X, Y), \quad \forall X, Y \in \mathbb{R}^{d \times n},$$

and Lyapunov function $\Psi(X, Y) := \|X - \bar{X}\|_F^2 + \|X - Y\|_F^2$ with $\bar{X} := \frac{1}{n} X \mathbf{1}\mathbf{1}^\top$, where \mathbb{E}_h denotes the expectation over internal randomness of averaging scheme h .

Example: Exact Averaging. Setting $X^+ = XW$ and $Y^+ = X^+$ gives an exact consensus averaging algorithm with mixing matrix W (Xiao and Boyd, 2004). It converges at the rate $c = \rho$, where ρ is an eigengap of mixing matrix W , defined in Assumption 1. Substituting it into the Algorithm 2 we recover D-PSGD algorithm, analyzed in (Lian et al., 2017).

Example: CHOCO-SGD. To recover CHOCO-SGD, we need to choose CHOCO-GOSSIP (Koloskova et al., 2019) as consensus averaging scheme, which is defined as $X^+ = X + \gamma Y(W - I)$ and $Y^+ = Y + Q(X^+ - Y)$ (in the main text we write \hat{X} instead of Y). This scheme converges with $c = \frac{\rho^2 \delta}{82}$. The

results from the main part can be recovered by substituting this $c = \frac{\rho^2 \delta}{82}$ in the more general results below. It is important to note that for Algorithm 1 given in the main text, the order of the communication part ① and the gradient computation part ② is exchanged. We did this to better illustrate that both these parts are independent and that they can be executed in parallel. The effect of this change can be captured by changing the initial values but does not affect the convergence rate.

A.2 Proof of Theorem 4.1

Lemma A.1. *Under Assumptions 1–2 the iterates of the Algorithm 2 with constant stepsize η satisfy*

$$\sum_{i=1}^n \left\| \bar{\mathbf{x}}^{(t)} - \mathbf{x}_i^{(t)} \right\|_2^2 \leq \eta^2 \frac{8nG^2}{c^2}.$$

Proof of Lemma A.1. Following exactly the same calculations as the first 9 lines in the proof of Lemma 21 from (Koloskova et al., 2019), we get a recursion

$$r_{t+1} \leq \left(1 - \frac{c}{2}\right) r_t + \frac{2}{c} \eta^2 A,$$

with $A = 2nG^2$, $r_t = \mathbb{E} \left\| X^{(t)} - \bar{X}^{(t)} \right\|^2 + \mathbb{E} \left\| X^{(t)} - Y^{(t)} \right\|^2$.

Verifying that $r_t \leq \eta^2 \frac{4A}{c^2}$ satisfy recursion completes the proof as $\mathbb{E} \left\| X^{(t)} - \bar{X}^{(t)} \right\|^2 \leq r_t$

$$r_{t+1} \leq \left(1 - \frac{c}{2}\right) r_t + \frac{2}{c} \eta^2 A \leq \left(1 - \frac{c}{2}\right) \eta^2 \frac{4A}{c^2} + \frac{2}{c} \eta^2 A = \eta^2 \frac{4A}{c^2}. \quad \square$$

Theorem A.2. *Under Assumptions 1–3 with constant stepsize $\eta = \sqrt{\frac{n}{T+1}}$ for $T \geq 64nL^2$, the averaged iterates $\bar{\mathbf{x}}^{(t)} = \frac{1}{n} \sum_{i=1}^n \mathbf{x}_i^{(t)}$ of Algorithm 2 satisfy:*

$$\frac{1}{T+1} \sum_{t=0}^T \left\| \nabla f(\bar{\mathbf{x}}^{(t)}) \right\|_2^2 \leq \frac{4 \left(f(\bar{\mathbf{x}}^{(0)}) - f^* \right) + 4\sigma^2 L}{\sqrt{n(T+1)}} + \frac{24G^2 nL}{(T+1)c^2}$$

where c denotes convergence rate of underlying averaging scheme.

The first term shows a linear speed up compared to SGD on one node, whereas the underlying averaging scheme affects only the second-order term. Substituting the convergence rate for exact averaging with W gives the rate $\mathcal{O}(1/\sqrt{nT} + n/(T\rho^2))$, which recovers the rate of D-PSGD (Lian et al., 2017).

CHOCO-SGD with the underlying CHOCO-GOSSIP averaging scheme converges at the rate $\mathcal{O}(1/\sqrt{nT} + n/(T\rho^4\delta^2))$. The dependence on ρ (eigengap of the mixing matrix W) is worse than in the exact case. This might either just be an artifact of our proof technique or a consequence of supporting arbitrary high compression.

Proof of Theorem A.2. By L -smoothness

$$\begin{aligned} \mathbb{E}_{t+1} f(\bar{\mathbf{x}}^{(t+1)}) &= \mathbb{E}_{t+1} f \left(\bar{\mathbf{x}}^{(t)} - \frac{\eta}{n} \sum_{j=1}^n \nabla F_j(\mathbf{x}_j^{(t)}, \xi_j^{(t)}) \right) \\ &\leq f(\bar{\mathbf{x}}^{(t)}) - \mathbb{E}_{t+1} \left\langle \nabla f(\bar{\mathbf{x}}^{(t)}), \frac{\eta}{n} \sum_{j=1}^n \nabla F_j(\mathbf{x}_j^{(t)}, \xi_j^{(t)}) \right\rangle + \mathbb{E}_{t+1} \frac{L}{2} \eta^2 \left\| \frac{1}{n} \sum_{j=1}^n \nabla F_j(\mathbf{x}_j^{(t)}, \xi_j^{(t)}) \right\|_2^2 \end{aligned}$$

To estimate the second term, we add and subtract $\nabla f(\bar{\mathbf{x}}^{(t)})$

$$\begin{aligned} -\eta \left\langle \nabla f(\bar{\mathbf{x}}^{(t)}), \frac{1}{n} \sum_{j=1}^n \nabla f_j(\mathbf{x}_j^{(t)}) \right\rangle &= -\eta \left\| \nabla f(\bar{\mathbf{x}}^{(t)}) \right\|^2 + \eta \left\langle \nabla f(\bar{\mathbf{x}}^{(t)}), \nabla f(\bar{\mathbf{x}}^{(t)}) - \frac{1}{n} \sum_{j=1}^n \nabla f_j(\mathbf{x}_j^{(t)}) \right\rangle \\ &\stackrel{(5), \gamma=1; (4)}{\leq} -\frac{\eta}{2} \left\| \nabla f(\bar{\mathbf{x}}^{(t)}) \right\|^2 + \frac{\eta}{2n} \sum_{j=1}^n \left\| \nabla f(\bar{\mathbf{x}}^{(t)}) - \nabla f_j(\mathbf{x}_j^{(t)}) \right\|^2 \end{aligned}$$

For the last term, we add and subtract $\nabla f(\bar{\mathbf{x}}^{(t)})$ and the sum of $\nabla f_j(\mathbf{x}_j^{(t)})$

$$\mathbb{E}_{t+1} \frac{L}{2} \eta^2 \left\| \frac{1}{n} \sum_{j=1}^n \nabla F_j(\mathbf{x}_j^{(t)}, \xi_j^{(t)}) \right\|_2^2 \stackrel{(3),(6)}{\leq} \frac{L\eta^2 \bar{\sigma}^2}{n} + \frac{2L\eta^2}{n} \sum_{j=1}^n \left\| f(\bar{\mathbf{x}}^{(t)}) - \nabla f_j(\mathbf{x}_j^{(t)}) \right\|_2^2 + 2L\eta^2 \left\| \nabla f(\bar{\mathbf{x}}^{(t)}) \right\|_2^2$$

Combining this together and using L -smoothness to estimate $\left\| f(\bar{\mathbf{x}}^{(t)}) - \nabla f_j(\mathbf{x}_j^{(t)}) \right\|_2^2$,

$$\mathbb{E}_{t+1} f(\bar{\mathbf{x}}^{(t+1)}) \leq f(\bar{\mathbf{x}}^{(t)}) - \eta \left(\frac{1}{2} - 2L\eta \right) \left\| \nabla f(\bar{\mathbf{x}}^{(t)}) \right\|_2^2 + \left(\frac{\eta L}{2n} + \frac{2L^2\eta^2}{n} \right) \sum_{j=1}^n \left\| \bar{\mathbf{x}}^{(t)} - \mathbf{x}_j^{(t)} \right\|_2^2 + \frac{L}{n} \eta^2 \bar{\sigma}^2.$$

Using Lemma 4.2 to bound the third term and using that $\eta \leq \frac{1}{8L}$ (this is because $\eta = \sqrt{\frac{n}{T+1}}$, $T \geq 64nL^2$)

$$\mathbb{E}_{t+1} f(\bar{\mathbf{x}}^{(t+1)}) \leq f(\bar{\mathbf{x}}^{(t)}) - \frac{\eta}{4} \left\| \nabla f(\bar{\mathbf{x}}^{(t)}) \right\|_2^2 + \frac{4\eta^3 LG^2}{c^2} + \eta^4 \frac{16L^2 G^2}{c^2} + \frac{L}{n} \eta^2 \bar{\sigma}^2,$$

Rearranging terms and averaging over t

$$\begin{aligned} \frac{1}{T+1} \sum_{t=0}^T \left\| \nabla f(\bar{\mathbf{x}}^{(t)}) \right\|_2^2 &\stackrel{(6)}{\leq} \frac{4}{\eta} \frac{1}{T+1} \sum_{t=0}^T \left(\mathbb{E} f(\bar{\mathbf{x}}^{(t)}) - \mathbb{E} f(\bar{\mathbf{x}}^{(t+1)}) \right) + \frac{16G^2\eta^2 L}{c^2} + \frac{4L}{n} \eta \bar{\sigma}^2 + 64\eta^3 \frac{nL^2 G^2}{c^2} \\ &\leq \frac{4}{\eta(T+1)} \left(f(\bar{\mathbf{x}}^{(0)}) - f^* \right) + \frac{4\eta \bar{\sigma}^2 L}{n} + \frac{16G^2\eta^2 L}{c^2} + \frac{64\eta^3 L^2 G^2}{c^2} \end{aligned}$$

Substituting $\eta = \sqrt{\frac{n}{T+1}}$ and using that $T \geq 64nL^2$ we get the statement of the theorem. \square

Proof of Corollary 4.3.

$$\begin{aligned} \frac{1}{T+1} \sum_{t=0}^T \frac{1}{n} \sum_{i=1}^n \left\| \nabla f(\mathbf{x}_i^{(t)}) \right\|_2^2 &\leq \frac{1}{T+1} \sum_{t=0}^T \frac{1}{n} \sum_{i=1}^n \left(2 \left\| \nabla f(\mathbf{x}_i^{(t)}) - \nabla f(\bar{\mathbf{x}}^{(t)}) \right\|_2^2 + 2 \left\| \nabla f(\bar{\mathbf{x}}^{(t)}) \right\|_2^2 \right) \\ &\leq \frac{1}{T+1} \sum_{t=0}^T \frac{1}{n} \sum_{i=1}^n \left(2L \left\| \mathbf{x}_i^{(t)} - \bar{\mathbf{x}}^{(t)} \right\|_2^2 + 2 \left\| \nabla f(\bar{\mathbf{x}}^{(t)}) \right\|_2^2 \right) \end{aligned}$$

where we used L -smoothness of f . Using Theorem 4.1 and Lemma 4.2

$$\frac{1}{T+1} \sum_{t=0}^T \frac{1}{n} \sum_{i=1}^n \left\| \nabla f(\mathbf{x}_i^{(t)}) \right\|_2^2 \leq \frac{8 \left(f(\bar{\mathbf{x}}^{(0)}) - f^* \right) + 8\bar{\sigma}^2 L}{\sqrt{n(T+1)}} + \frac{64G^2 nL}{(T+1)c^2}. \quad \square$$

A.3 Convergence for Arbitrary T

The previous result holds only for T larger than $64nL^2$. This is not necessary and can be relaxed.

Theorem A.3. *Under Assumptions 2, 1 with constant stepsize η and the consensus stepsize $\gamma := \frac{\rho^2 \delta}{16\rho + \rho^2 + 4\beta^2 + 2\rho\beta^2 - 8\rho\delta}$ where $\beta = \|I - W\|_2 \in [0, 2]$ Algorithm 2 converges at the speed*

$$\frac{1}{T+1} \sum_{t=0}^T \left\| \nabla f(\bar{\mathbf{x}}^{(t)}) \right\|_2^2 \leq \frac{2}{\eta(T+1)} \left(f(\bar{\mathbf{x}}^{(0)}) - f^* \right) + \frac{\eta G^2 L}{n} + \frac{8G^2 \eta^2 L}{c^2},$$

where $\bar{\mathbf{x}}^{(t)} = \sum_{i=1}^n \mathbf{x}_i^{(t)}$ and c is convergence rate of underlying averaging scheme.

In contrast to Theorem A.2, this rate holds for any T , however the first term is worse than in Theorem A.2 because $\bar{\sigma}^2$ is usually much smaller than G^2 .

Proof of Theorem A.3. By L -smoothness

$$\begin{aligned}
\mathbb{E}_{t+1} f(\bar{\mathbf{x}}^{(t+1)}) &= \mathbb{E}_{t+1} f\left(\bar{\mathbf{x}}^{(t)} - \frac{\eta}{n} \sum_{j=1}^n \nabla F_j(\mathbf{x}_j^{(t)}, \xi_j^{(t)})\right) \\
&\leq f(\bar{\mathbf{x}}^{(t)}) - \mathbb{E}_{t+1} \left\langle \nabla f(\bar{\mathbf{x}}^{(t)}), \frac{\eta}{n} \sum_{j=1}^n \nabla F_j(\mathbf{x}_j^{(t)}, \xi_j^{(t)}) \right\rangle + \mathbb{E}_{t+1} \frac{L}{2} \eta^2 \left\| \frac{1}{n} \sum_{j=1}^n \nabla F_j(\mathbf{x}_j^{(t)}, \xi_j^{(t)}) \right\|_2^2 \\
&\stackrel{(3)}{\leq} f(\bar{\mathbf{x}}^{(t)}) - \eta \left\langle \nabla f(\bar{\mathbf{x}}^{(t)}), \frac{1}{n} \sum_{j=1}^n \nabla f_j(\mathbf{x}_j^{(t)}) \right\rangle + \frac{L}{2n} \eta^2 G^2 \\
&= f(\bar{\mathbf{x}}^{(t)}) - \eta \left\| \nabla f(\bar{\mathbf{x}}^{(t)}) \right\|_2^2 + \eta \left\langle \nabla f(\bar{\mathbf{x}}^{(t)}), \nabla f(\bar{\mathbf{x}}^{(t)}) - \frac{1}{n} \sum_{j=1}^n \nabla f_j(\mathbf{x}_j^{(t)}) \right\rangle + \frac{L}{2n} \eta^2 G^2 \\
&\stackrel{(5),(4)}{\leq} f(\bar{\mathbf{x}}^{(t)}) - \eta \left\| \nabla f(\bar{\mathbf{x}}^{(t)}) \right\|_2^2 + \frac{\alpha\eta}{2} \left\| \nabla f(\bar{\mathbf{x}}^{(t)}) \right\|_2^2 + \frac{\eta}{2\alpha n} \sum_{j=1}^n \left\| \nabla f_j(\bar{\mathbf{x}}^{(t)}) - \nabla f_j(\mathbf{x}_j^{(t)}) \right\|_2^2 + \frac{L}{2n} \eta^2 G^2 \\
&\leq f(\bar{\mathbf{x}}^{(t)}) - \eta \left(1 - \frac{\alpha}{2}\right) \left\| \nabla f(\bar{\mathbf{x}}^{(t)}) \right\|_2^2 + \frac{\eta L}{2\alpha n} \sum_{j=1}^n \left\| \bar{\mathbf{x}}^{(t)} - \mathbf{x}_j^{(t)} \right\|_2^2 + \frac{L}{2n} \eta^2 G^2
\end{aligned}$$

Using Lemma 4.2 we can bound the last term

$$\mathbb{E}_{t+1} f(\bar{\mathbf{x}}^{(t+1)}) \leq f(\bar{\mathbf{x}}^{(t)}) - \eta \left(1 - \frac{\alpha}{2}\right) \left\| \nabla f(\bar{\mathbf{x}}^{(t)}) \right\|_2^2 + \frac{4G^2\eta^3 L}{\alpha c^2} + \frac{L}{2n} \eta^2 G^2$$

Rearranging terms, taking $\alpha = 1$ and averaging over t we are getting statement of the theorem

$$\begin{aligned}
\frac{1}{T+1} \sum_{t=0}^T \left\| \nabla f(\bar{\mathbf{x}}^{(t)}) \right\|_2^2 &\stackrel{(6)}{\leq} \frac{2}{\eta} \frac{1}{T+1} \sum_{t=0}^T \left(\mathbb{E} f(\bar{\mathbf{x}}^{(t)}) - \mathbb{E} f(\bar{\mathbf{x}}^{(t+1)}) \right) + \frac{8G^2\eta^2 L}{c^2} + \frac{L}{n} \eta G^2 \\
&\leq \frac{2}{\eta(T+1)} \left(f(\bar{\mathbf{x}}^{(0)}) - f^* \right) + \frac{\eta G^2 L}{n} + \frac{8G^2\eta^2 L}{c^2} \quad \square
\end{aligned}$$

Corollary A.4 (Convergence of local weights $\mathbf{x}_i^{(t)}$). *Under Assumptions 2, 1, algorithm 1 with $\eta = \sqrt{\frac{n}{T+1}}$ converges at the speed*

$$\frac{1}{T+1} \sum_{t=0}^T \frac{1}{n} \sum_{i=1}^n \left\| \nabla f(\mathbf{x}_i^{(t)}) \right\|_2^2 \leq \frac{4 \left(f(\bar{\mathbf{x}}^{(0)}) - f^* \right) + 2G^2 L}{\sqrt{n(T+1)}} + \frac{16G^2 n(L+1)}{c^2(T+1)}.$$

Proof.

$$\begin{aligned}
\frac{1}{T+1} \sum_{t=0}^T \frac{1}{n} \sum_{i=1}^n \left\| \nabla f(\mathbf{x}_i^{(t)}) \right\|_2^2 &\leq \frac{1}{T+1} \sum_{t=0}^T \frac{1}{n} \sum_{i=1}^n \left((1+\alpha) \left\| \nabla f(\mathbf{x}_i^{(t)}) - \nabla f(\bar{\mathbf{x}}^{(t)}) \right\|_2^2 + (1+\alpha^{-1}) \left\| \nabla f(\bar{\mathbf{x}}^{(t)}) \right\|_2^2 \right) \\
&\leq \frac{1}{T+1} \sum_{t=0}^T \frac{1}{n} \sum_{i=1}^n \left(L(1+\alpha) \left\| \mathbf{x}_i^{(t)} - \bar{\mathbf{x}}^{(t)} \right\|_2^2 + (1+\alpha^{-1}) \left\| \nabla f(\bar{\mathbf{x}}^{(t)}) \right\|_2^2 \right)
\end{aligned}$$

where we used L -smoothness of f . This holds for $\forall \alpha > 0$. Using Theorem A.3 and Lemma A.1 and

setting $\alpha = 1$

$$\begin{aligned}
\frac{1}{T+1} \sum_{t=0}^T \frac{1}{n} \sum_{i=1}^n \left\| \nabla f(\mathbf{x}_i^{(t)}) \right\|_2^2 &\leq 2 \frac{8G^2\eta^2}{c^2} + 2 \frac{2}{\eta(T+1)} \left(f(\bar{\mathbf{x}}^{(0)}) - f^\star \right) + 2 \frac{\eta G^2 L}{n} + 2 \frac{8G^2\eta^2 L}{c^2} = \\
&= 2 \frac{8G^2\eta^2(L+1)}{c^2} + 2 \frac{2}{\eta(T+1)} \left(f(\bar{\mathbf{x}}^{(0)}) - f^\star \right) + 2 \frac{\eta G^2 L}{n} = \\
&= 2 \frac{8G^2 n(L+1)}{c^2(T+1)} + 2 \frac{2}{\sqrt{n(T+1)}} \left(f(\bar{\mathbf{x}}^{(0)}) - f^\star \right) + 2 \frac{G^2 L}{\sqrt{n(T+1)}}.
\end{aligned}$$

where we set $\eta = \sqrt{\frac{n}{T+1}}$. □

B Useful Inequalities

Lemma B.1. For arbitrary set of n vectors $\{\mathbf{a}_i\}_{i=1}^n$, $\mathbf{a}_i \in \mathbb{R}^d$

$$\left\| \sum_{i=1}^n \mathbf{a}_i \right\|^2 \leq n \sum_{i=1}^n \|\mathbf{a}_i\|^2. \quad (4)$$

Lemma B.2. For given two vectors $\mathbf{a}, \mathbf{b} \in \mathbb{R}^d$

$$2 \langle \mathbf{a}, \mathbf{b} \rangle \leq \gamma \|\mathbf{a}\|^2 + \gamma^{-1} \|\mathbf{b}\|^2, \quad \forall \gamma > 0. \quad (5)$$

Lemma B.3. For given two vectors $\mathbf{a}, \mathbf{b} \in \mathbb{R}^d$

$$\|\mathbf{a} + \mathbf{b}\|^2 \leq (1 + \alpha) \|\mathbf{a}\|^2 + (1 + \alpha^{-1}) \|\mathbf{b}\|^2, \quad \forall \alpha > 0. \quad (6)$$

This inequality also holds for the sum of two matrices $A, B \in \mathbb{R}^{n \times d}$ in Frobenius norm.

C Compression Schemes

We implement the compression schemes detailed below.

- gsgd_b (Alistarh et al., 2017). The unbiased $\text{gsgd}_b: \mathbb{R}^d \rightarrow \mathbb{R}^d$ compression operator (for $b > 1$) is given as

$$\text{gsgd}_b(\mathbf{x}) := \|\mathbf{x}\|_2 \cdot \text{sig}(\mathbf{x}) \cdot 2^{-(b-1)} \cdot \left\lfloor \frac{2^{(b-1)} \|\mathbf{x}\|_2}{\|\mathbf{x}\|_2} + \mathbf{u} \right\rfloor$$

where $\mathbf{u} \sim_{u.a.r.} [0, 1]^d$ is a random dithering vector and $\text{sig}(\mathbf{x})$ assigns the element-wise sign: $(\text{sig}(\mathbf{x}))_i = 1$ if $(\mathbf{x})_i \geq 0$ and $(\text{sig}(\mathbf{x}))_i = -1$ if $(\mathbf{x})_i < 0$. As the value in the right bracket will be rounded to an integer in $\{0, \dots, 2^{(b-1)} - 1\}$, each coordinate can be encoded with at most $(b-1) + 1$ bits (1 for the sign). For more efficient encoding schemes cf. (Alistarh et al., 2017).

A biased version is given as

$$\text{gsgd}_b(\mathbf{x}) := \frac{\|\mathbf{x}\|_2}{\tau} \cdot \text{sig}(\mathbf{x}) \cdot 2^{-(b-1)} \cdot \left\lfloor \frac{2^{(b-1)} \|\mathbf{x}\|_2}{\|\mathbf{x}\|_2} + \mathbf{u} \right\rfloor$$

for $\tau = 1 + \min \left\{ \frac{d}{2^{2(b-1)}}, \frac{\sqrt{d}}{2^{(b-1)}} \right\}$ and is a $\delta = \frac{1}{\tau}$ compression operator (Koloskova et al., 2019).

- random_a (Wangni et al., 2018). Let $\mathbf{u} \in \{0, 1\}^d$ be a masking vector, sampled uniformly at random from the set $\{\mathbf{u} \in \{0, 1\}^d : \|\mathbf{u}\|_1 = \lfloor ad \rfloor\}$. Then the unbiased $\text{random}_a: \mathbb{R}^d \rightarrow \mathbb{R}^d$ operator is defined as

$$\text{random}_a(\mathbf{x}) := \frac{d}{\lfloor ad \rfloor} \cdot \mathbf{x} \odot \mathbf{u}.$$

The biased version is given as

$$\text{random}_a(\mathbf{x}) := \mathbf{x} \odot \mathbf{u},$$

and is a $\delta = a$ compression operator (Stich et al., 2018).

Only $32\lfloor ad \rfloor$ bits are required to send $\text{random}_a(\mathbf{x})$ to another node—all the values of non-zero entries (we assume that entries are represented as `float32` numbers). Receiver can recover positions of these entries if it knows the random seed of uniform sampling operator used to select these entries. This random seed could be communicated once on preprocessing stage (before starting the algorithm).

- top_a (Alistarh et al., 2018; Stich et al., 2018). The biased $\text{top}_a: \mathbb{R}^d \rightarrow \mathbb{R}^d$ operator is defined as

$$\text{top}_a(\mathbf{x}) := \mathbf{x} \odot \mathbf{u}(\mathbf{x}),$$

where $\mathbf{u}(\mathbf{x}) \in \{0, 1\}^d$, $\|\mathbf{u}\|_1 = \lfloor ad \rfloor$ is a masking vector with $(\mathbf{u})_i = 1$ for indices $i \in \pi^{-1}(\{1, \dots, \lfloor ad \rfloor\})$ where the permutation π is such that $|(\mathbf{x})_{\pi(1)}| \geq |(\mathbf{x})_{\pi(2)}| \geq \dots \geq |(\mathbf{x})_{\pi(d)}|$. The top_a operator is a $\delta = a$ compression operator (Stich et al., 2018).

In the case of top_a compression $2 \cdot 32\lfloor ad \rfloor$ bits are required because along with the values we need to send positions of these values.

- sign (Bernstein et al., 2018; Karimireddy et al., 2019). The biased (scaled) $\text{sign}: \mathbb{R}^d \rightarrow \mathbb{R}$ compression operator is defined as

$$\text{sign}(\mathbf{x}) := \frac{\|\mathbf{x}\|_1}{d} \cdot \text{sgn}(\mathbf{x}).$$

The sign operator is a $\delta = \frac{\|\mathbf{x}\|_1^2}{d\|\mathbf{x}\|_2^2}$ compression operator (Karimireddy et al., 2019).

In total for the sign compression we need to send only $d + 32$ bits—one bit for every entry in \mathbf{x} and 32 bits for $\|\mathbf{x}\|_1$.

D CHOCO-SGD with Momentum

Algorithm 3 below demonstrates how to combine CHOCO-SGD with weight decay and momentum. Nesterov momentum can be analogously adapted for our decentralized setting.

Algorithm 3 CHOCO-SGD (Koloskova et al., 2019) with Momentum

input: Initial values $\mathbf{x}_i^{(0)} \in \mathbb{R}^d$ on each node $i \in [n]$, consensus stepsize γ , SGD stepsize η , communication graph $G = ([n], E)$ and mixing matrix W , initialize $\hat{\mathbf{x}}_i^{(0)} := \mathbf{0} \forall i \in [n]$, weight decay factor λ , momentum factor β , local momentum memory $\mathbf{m}_i^{(0)} := \mathbf{0} \forall i \in [n]$

- 1: **for** t **in** $0 \dots T - 1$ **do** *{in parallel for all workers $i \in [n]$ }*
- 2: $\mathbf{x}_i^{(t)} := \mathbf{x}_i^{(t-\frac{1}{2})} + \gamma \sum_{j: \{i,j\} \in E} w_{ij} (\hat{\mathbf{x}}_j^{(t)} - \hat{\mathbf{x}}_i^{(t)})$ \triangleleft modified gossip averaging
- 3: $\mathbf{q}_i^{(t)} := Q(\mathbf{x}_i^{(t)} - \hat{\mathbf{x}}_i^{(t)})$ \triangleleft compression
- 4: **for** neighbors $j: \{i, j\} \in E$ (including $\{i\} \in E$) **do**
- 5: Send $\mathbf{q}_i^{(t)}$ and receive $\mathbf{q}_j^{(t)}$ \triangleleft communication
- 6: $\hat{\mathbf{x}}_j^{(t+1)} := \mathbf{q}_j^{(t)} + \hat{\mathbf{x}}_j^{(t)}$ \triangleleft local update
- 7: **end for**
- 8: Sample $\xi_i^{(t)}$, compute gradient $\mathbf{g}_i^{(t)} := \nabla F_i(\mathbf{x}_i^{(t)}, \xi_i^{(t)})$
- 9: $\mathbf{v}_i^{(t+1)} := (\mathbf{g}_i^{(t)} + \lambda \mathbf{x}_i^{(t)}) + \beta \mathbf{v}_i^{(t)}$ \triangleleft local momentum with weight decay
- 10: $\mathbf{x}_i^{(t+\frac{1}{2})} := \mathbf{x}_i^{(t)} - \eta \mathbf{v}_i^{(t+1)}$ \triangleleft stochastic gradient update
- 11: **end for**

E Model Training and Tuned Hyperparameters

We precise the procedure of model training as well as the hyper-parameter tuning in this section.

For all algorithms, we gradually warmup (Goyal et al., 2017) the learning rate from a relative small value (0.1) to the fine-tuned initial learning rate for the first 5 training epochs. During the training procedure, the tuned initial learning rate is decayed by the factor of 10 when accessing 50% and 75% of the total training epochs. The learning rate is tuned by finding the optimal learning rate per sample $\hat{\eta}$, where the learning rate (used locally) is determined by a linear scaling rule (i.e., degree of node $\times \hat{\eta} \times$ per node mini-batch size).

The optimal $\hat{\eta}$ is searched in a pre-defined grid and we ensure that the best performance was contained in the middle of the grids. For example, if the best performance was ever at one of the extremes of the grid, we would try new grid points. Same searching logic applies to the consensus stepsize.

Table 3 demonstrates the fine-tuned hyperparameters of CHOCO-SGD for training ResNet-20 on Cifar10. Table 4 demonstrates the fine-tuned hyperparameters of CHOCO-SGD for training ResNet-20/LSTM on a social network topology.

Table 3: Tuned hyper-parameters of CHOCO-SGD for training ResNet-20 on Cifar10, corresponding to the ring topology with 8 nodes in Table 1. We randomly split the training data between nodes and shuffle it after every epoch. The per node mini-batch size is 128 and the degree of each node is 3.

Compression schemes	Learning rate	Consensus stepsize
QSGD (16-bit)	1.60	0.2
QSGD (8-bit)	0.96	0.2
QSGD (4-bit)	1.60	0.075
QSGD (2-bit)	0.96	0.025
Sparsification (random-50%)	2.40	0.45
Sparsification (random-10%)	1.20	0.075
Sparsification (random-1%)	0.48	0.00625
Sparsification (top-50%)	1.60	0.45
Sparsification (top-10%)	1.60	0.15
Sparsification (top-1%)	1.20	0.0375
Sign+Norm	1.60	0.45

Table 4: Tuned hyper-parameters of CHOCO-SGD, corresponding to the social network topology with 32 nodes in Table 2. We randomly split the training data between the nodes and keep this partition fixed during the entire training (no shuffling). The per node mini-batch size is 32 and the maximum degree of the node is 14.

Configuration	Base learning rate (before scaling by node degree)	Consensus stepsize
ResNet-20, Cifar10, Sign+Norm	0.13	0.3
LSTM, WikiText-2, Sign+Norm	0.20	0.8

F Additional Plots

We additionally plot the learning curve for the social network topology in Figure. 4 and Figure. 5.

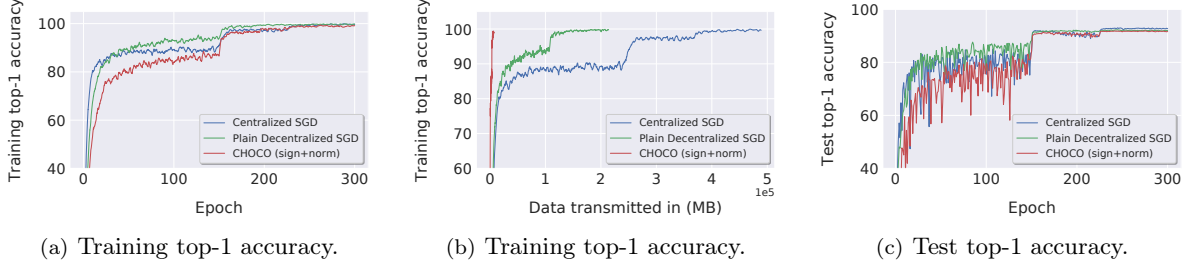


Figure 4: Training **ResNet-20** on **CIFAR-10** with decentralized algorithm on a real world social network topology. The topology has 32 nodes and we assume each node can only access a disjoint subset of the whole dataset. The local mini-batch size is 32.

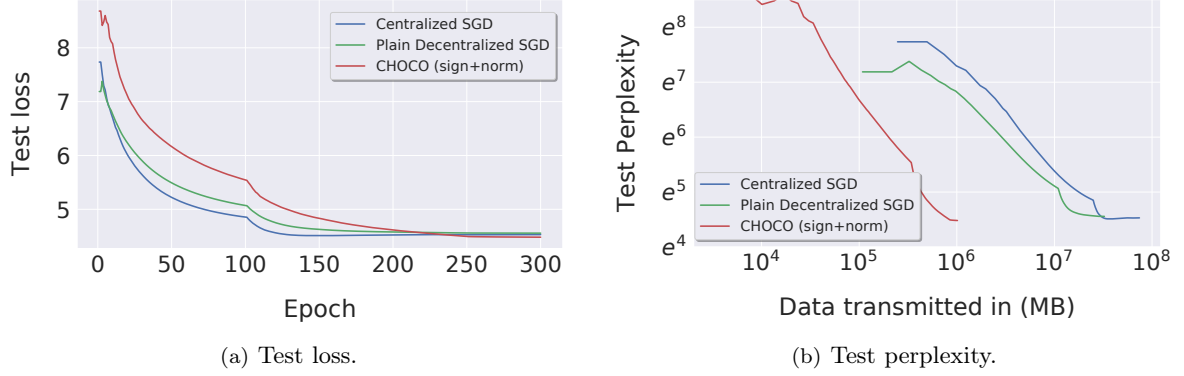


Figure 5: Training **LSTM** on **WikiText2** with decentralized algorithm on a real world social network topology. The topology has 32 nodes and we assume each node can only access a disjoint subset of the whole dataset. The local mini-batch size is 32.

We additionally provide plots for training top-1, top-5 accuracy and test top-5 accuracy for the datacenter experiment in Figure 6.

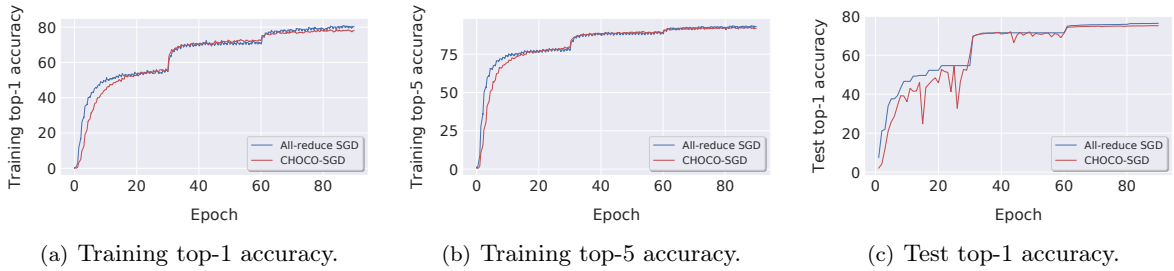


Figure 6: Large-scale training: **ResNet-50** on **ImageNet** in the datacenter.